CAV2021
11th International Symposium on Cavitation
May 10-13, 2021, Daejon, Korea

On the cloud interaction parameter and its connections with the coherence and discrete spectrum of bubble cloud dynamics

Kazuki Maeda[1]*, Daniel Fuster[2]

[1]Center for Turbulence Research, Stanford University
[2]Sorbonne Universit´e, Centre National de la Recherche Scientifique (CNRS)

Abstract: We present an analysis and characterization of the coherent dynamics of bubble clouds. The study is two folds. First, through analysis of the Rayleigh-Plesset equation, we systematically show that the diagonal dominance of the virtual-mass matrix of the system of Lagrangian bubbles is parametrized by the cloud interaction parameter that controls the coherent dynamics of bubbles (d'Agostino and Brennen, *J. Fluid. Mech*., 1989). Second, based on this insight, we introduce the principal component analysis (PCA) of a time series of Lagrangian bubble dynamic data. Through PCA of test data, we show that the variance of the principal component can be directly correlated with the interaction parameter when a proper normalization (weighting) of the data is made. We further show that the incoherence of the bubble dynamics due to the initial polydispersity and the nonlinear oscillations of bubbles can appear in the slope of the decay of the variances. These results may help further understand the interaction parameter as well as suggest that the weighted PCA can be a simple, systematic means to characterize the coherent dynamics of bubbles with various parameters.

Keywords: Cloud cavitation, coherence, many body physics, data analysis

1. Introduction

The dynamics of cavitation bubble clouds are of critical importance in medical and industrial applications as well as in sonoluminescence and sonochemistry. Challenges remain in understanding and controlling the dynamics; the oscillations of microscopic bubbles in a cloud are subjected many-body interactions and often intractable with measurements. Previous studies identified a non-dimensional parameter which dictates the coherent dynamics of bubble clouds, *the cloud interaction parameter*. The parameter can be derived from the scaling analysis of the governing equations a-priori and was used to characterize dynamics including in-phase, coherent oscillations of bubbles and spatially biased, localized excitation of bubbles in the cloud [1,2]. Further understanding and quantifying these coherent features may enable reduced-order representation of the complex dynamics for modeling and control. To this end, questions remain in terms of (1) the validity of using the single parameter to characterize the complex dynamics that involve many factors such as the cloud shape, polydispersity, profile of excitation (forcing) pressure, and (2) availability of further systematic methods to extract the coherent features from data.

In the present study, we address these questions through a twofold approach. First, we revisit the connection between the Lagrangian representation of the bubble dynamics using the Rayleigh-Plesset (R-P) equation. We show that the interaction parameter controls the diagonal dominance of the virtual-mass matrix of the R-P equation, and thus represents the dominance of the inter-bubble interactions in the cloud. Second, based on this knowledge, we explore the use of the principal component analysis (PCA) of the data matrix containing the discrete evolution of variables associated with Lagrangian bubbles, as a means to extract and characterize the coherent dynamics of bubbles from data. The use of PCA here is primarily inspired by the recent data-science approaches to analyze many-body Hamiltonian systems [3]. We perform several sets of numerical experiments. We first perform PCA of bubble dynamic data under linear periodic oscillations, using various weighting methods. We show that, with a proper normalization (weighting) of the data, the PCA can account for the contribution of the inter-bubble interactions in a manner consistent with the R-P equation. We identify that the interaction parameter is correlated with the variance of the first principal component. We further show that increasing both the polydispersity of bubbles in the cloud and the forcing amplitude can lead to a slower decay of the variances of the following components (discrete spectrum), and therefore that the

* Corresponding Author: kemaeda@stanford.edu

PCA can quantify the coherence of the bubble dynamics. These results further help understand the interaction parameter as well as suggest that the PCA can be a simple, systematic means to characterize the dynamics of bubble clouds from data.

2. Methods

3.1. Rayleigh-Plesset equation and the cloud interaction parameter

We consider the Rayleigh-Plesset equation formulated for multiple bubbles under mutual interactions.

$$R_i\ddot{R}_i + \frac{3}{2}\dot{R}_i^2 = \frac{p_i - p_e}{\rho} - \sum_{k\neq i}^{N_b}\frac{R_k}{r_{ik}}\left(R_k\ddot{R}_k + 2\dot{R}_k^2\right) \quad (1), \qquad p_i = \left(p_0 + \frac{2\sigma}{R_{i0}}\right)\left(\frac{R_{i0}}{R_i}\right)^{3\gamma} - \frac{2\sigma}{R_i} - \frac{4\nu\dot{R}_i}{R_i} \quad (2).$$

Note that R_i is the radius of the i-th bubble, R_{i0} is that at equilibrium, r_{ik} is the distance between bubble-i and bubble-k, p_0 is the pressure of liquid at equilibrium, p_e is the time-dependent pressure at infinity, σ is the surface tension, ν is the dynamic viscosity of liquid, γ is the specific heat ratio of the gas, and ρ is the density of liquid. The physical parameters of liquid are chosen for ambient water. The R-P equation can be expressed using the following vector form of equations as

$$\boldsymbol{M}(\boldsymbol{r},\boldsymbol{x})\dot{\boldsymbol{q}} = \boldsymbol{f}(\boldsymbol{q},\boldsymbol{r},\boldsymbol{x}) + \boldsymbol{s}, \;\; \dot{\boldsymbol{r}} = \boldsymbol{q}. \quad (3)$$

where $\boldsymbol{x}$ denotes the coordinates (position) of the bubbles and

$$M_{ij} = \begin{cases} R_i, & i = j \\ \dfrac{R_i^2}{r_{ij}}, & i \neq j \end{cases}, \quad q_i = \dot{R}_i, \quad r_i = R_i, \quad s_i = \frac{p_i - p_e}{\rho}.$$

(3) is regarded as an equation of motion for the bubble radius. Further discussions on the R-P equation can be elsewhere [4]. $\boldsymbol{M}$ is weighting the acceleration of the bubble radius and can be regarded as the added-mass matrix of the system. The property of $\boldsymbol{M}$ is critical for the solution of the pseudo-linear system (3). The non-diagonal entries of $\boldsymbol{M}$ represent the contribution of the inter-bubble interactions on the accelerations of the radii of the bubbles. To mathematically quantify this contribution, we consider the diagonal dominance; $\boldsymbol{M}$ is *diagonally dominant* if

$$\sum_i^{N_b} R_i > \sum_i^{N_b}\sum_{k\neq i}^{N_b}\frac{R_i^2}{r_{ik}}.$$

When the bubble dynamics are assumed stationary, by scaling the radius and the inter-bubble distance with the mean, $<R>$, and with the cloud size, L, this condition can be expressed as $1 > \frac{N_b<R>}{L} \sim B$, where B is the cloud interaction parameter. Therefore, B is a measure of the diagonal dominance of $\boldsymbol{M}$. Physically speaking, it has been shown that B controls the kinetic energy of liquid induced by the oscillations of the bubbles. To further assess the connections of K and $\boldsymbol{M}$, we express the energy using $\boldsymbol{M}$ as

$$K = \boldsymbol{q}^{\mathrm{T}}\boldsymbol{T}\boldsymbol{q} \quad (4), \qquad \text{where } \boldsymbol{T} = \boldsymbol{Q}\boldsymbol{M} \text{ and } Q_{ij} = \begin{cases} 2\pi\rho R_i^2, & i = j \\ 0, & i \neq j \end{cases}.$$

With the same scaling, the condition for the diagonal dominance of $\boldsymbol{T}$ is the same as that of $\boldsymbol{A}$. It is shown that B measures the contribution of the non-diagonal components of $\boldsymbol{A}$ to the kinetic energy.

3.2. Principal component analysis (PCA)

Assume that the time series of the radius and the radial velocity of each bubble in the cloud, $\boldsymbol{Q} = [\boldsymbol{q}^1, \boldsymbol{q}^2, \ldots, \boldsymbol{q}^L]$ and $\boldsymbol{R} = [\boldsymbol{r}^1, \boldsymbol{r}^2, \ldots, \boldsymbol{r}^L]$, are available as a solution of equation (3). The dominant features of the data can be extracted using the PCA. We use the singular value decomposition (SVD) to perform the PCA.

$$\boldsymbol{LQ} = \boldsymbol{U\Sigma V}^*, \quad (5)$$

* Corresponding Author: kemaeda@stanford.edu

where Σ is a rectangular diagonal matrix whose diagonal entries correspond to the principal components. $\boldsymbol{L}$ is a weighting matrix. $\boldsymbol{L}$ is arbitrary from the data science perspective. For physical systems, $\boldsymbol{L}$ can be chosen such that the variance of the principal components represents physically meaningful quantities. PCA of spatio-temporal Eulerian flow field data is often denoted as proper orthogonal decomposition (POD). In the POD, $\boldsymbol{L}$ is chosen such that the inner product $(\boldsymbol{Lq})^*\boldsymbol{Lq}$ represents the system's energy [5]. In the present study, we consider two choices of $\boldsymbol{L}$, namely $\boldsymbol{L}_1$ and $\boldsymbol{L}_2$. $\boldsymbol{L}_1$ is defined as the following diagonal matrix.

$$L_{1\,ij} = \begin{cases} \sqrt{2\pi\rho\bar{R}_i^3}, & i = j \\ 0, & i \neq j \end{cases},$$

where $(\bar{\ })$ denotes the time average during the time window of the data. $\boldsymbol{L}_2$ is defined through the Cholesky decomposition of the weighting matrix that is used to obtain K in equation (4).

$$\bar{\boldsymbol{T}} = \boldsymbol{L}_2\boldsymbol{L}_2^*,\ \ \bar{T}_{ij} = \begin{cases} 2\pi\rho\bar{R}_i^3, & i = j \\ 2\pi\rho\dfrac{\bar{R}_i^2\bar{R}_j^2}{r_{ik}}, & i \neq j \end{cases},$$

With $\boldsymbol{L}_1$, the inner product $(\boldsymbol{Lq})^*\boldsymbol{Lq}$ becomes the measure of the energy induced by each single bubble without consideration of the inter-bubble interaction**.** The POD typically uses this diagonal form of weighting matrixes. With $\boldsymbol{L}_2$, the product provides for an approximation of K and therefore accounts for the system's energy induced by the many-body interaction represented by the non-diagonal entries of $\boldsymbol{M}$.

3. Results

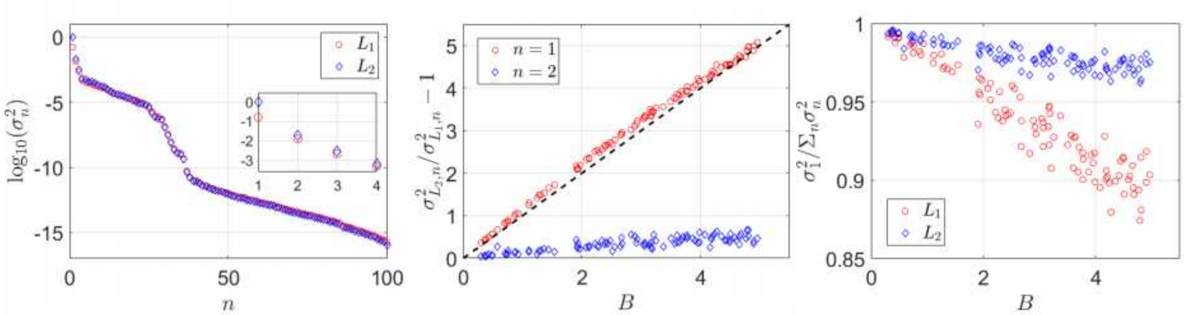

(a) (b) (c)

Figure 1. (a) PCA variance obtained with the two distinct weighting matrixes, $\boldsymbol{L}_1$ and $\boldsymbol{L}_2$. The results are normalized by σ^2_1 obtained with $\boldsymbol{L}_2$. (b) Ratio of the PCA variances obtained with the two weights as a function of B, for the first and second principal components. (c) Ratio of the first PCA variance to the total variance as a function of B, for $\boldsymbol{L}_1$ and $\boldsymbol{L}_2$.

We perform several sets of numerical experiments. First, we excite a spherical bubble cloud including 100 monodisperse bubbles with R_0=10 um with external pressure $p_e = p_0 + p_a\sin(2\pi ft)$, where p_0 = 1 atm, p_a = 10^3 Pa, and f = 1 MHz. The cloud radius is varied at O(0.1-1) mm such that B satisfies $0 < B < 5$. Figure 1a compared the PCA variances obtained using $\boldsymbol{L}_1$ and $\boldsymbol{L}_2$, for a cloud with B=5. The sets of the variances are nearly identical with each other, except that the first variance is greater with $\boldsymbol{L}_2$. Figure 1b shows the ratio of the variances obtained using $\boldsymbol{L}_1$ and $\boldsymbol{L}_2$ for the first and second principal components, for clouds with various values of B. The ratio of the first variance is linear to B, while the second variance is nearly zero. Figure 1c shows the ratio of the first PCA variance to the total variance as a function of B, for the same set of bubble clouds. For the case with $\boldsymbol{L}_2$, the first variance occupies a portion greater than 95% of the total variance. These results indicate that the coherent oscillations is captured by the first principal component, and that the variance of the first component obtained with $\boldsymbol{L}_2$ can be scaled with B.

* Corresponding Author: kemaeda@stanford.edu

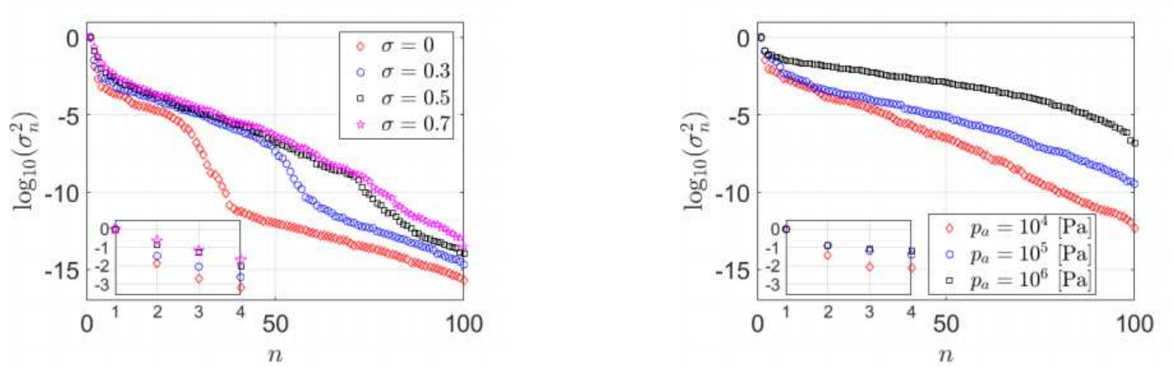

(**a**) (**b**)

Figure 2. (a) PCA variance obtained with L_2, for various values of polydispersity of bubble clouds with B = 5. (b) PCA variance obtained with L_2, for polydisperse bubble clouds with B = 5 excited by various amplitudes of the external pressure.

Second, we excite a spherical bubble cloud including 100 polydisperse bubbles with B = 5.The bubble size follows the lognormal distribution with a reference radius of 10 um and a standard deviation σ. Four cases are simulated with σ = 0, 0.3, 0.5, and 0.7. With increasing σ, we include bubbles with wider a range of characteristic frequencies. The same external pressure is used as the previous case. Figure 2a shows the obtained PCA variances. The decay of the variance becomes less steep with increasing the polydispersity.

Third, we excite the same bubble cloud with σ = 0.7 and with various values of p_a: p_a = 10^4, 10^5, and 10^6 Pa. With increasing p_a, the bubble dynamics become more nonlinear. Figure 2b shows the obtained variances. The decay of the variance becomes less steep with increasing the amplitude of the forcing pressure. The results of the second and the third case indicate that increasing the polydispersity and the forcing pressure can enhance the incoherence of the bubble oscillations (the first principal component becomes less dominant), and this enhancement is captured by the spectral decay of PCA.

4. Conclusions

In conclusion, we established the connections between the cloud interaction parameter and the PCA of Lagrangian bubble dynamics data. We identified that the parameter is a measure of the diagonal dominance of the added-mass matrix that appears in the R-P equation for multiple bubbles. The PCA can capture the effect of the many-body interactions of bubbles when a proper weighting strategy is used. We showed that the variance of the principal component is correlated with the interaction parameter. Furthermore, this PCA can inform on the incoherence of the oscillations of bubbles, which can be enhanced by the polydispersity and the forcing amplitude, through spectral decay. Future work includes further assessing the capabilities of the PCA to characterize the bubble cloud dynamics with various parameters.

Acknowledgments: K.M worked on the initial part of this study while visiting Sorbonne Universit´e from California Institute of Technology (Caltech). He gratefully acknowledges support by Sorbonne Universit´e, Caltech, and Center for Turbulence Research.

References

1. d'Agostino, L. and Brennen, CE (1989)., J. Fluid. Mech., 199, 155-176.
2. Maeda, K. and Colonius T (2018)., J. Fluid. Mech., 862, 1105.
3. Lloyd, S., Mohseni, M., and Rebentrost P (2014)., Nat. Phys., 10(9), 631-633.
4. Maeda, K (2018)., PhD Thesis, Appendix A., Caltech.
5. Rowley, CW (2005)., Int. J. Bifurc. Chaos Appl. Sci. Eng., 15(03), pp.997-1013.

* Corresponding Author: kemaeda@stanford.edu